

## NON-INTERCEPTING DIAGNOSTIC FOR THE HIF NEUTRALIZED TRANSPORT EXPERIMENT\*

P. K. Roy <sup>#</sup>, S. Eylon, R. Hannink, E. Henestroza, J. Ludvig, D. Shuman, and S. S. Yu  
Lawrence Berkeley National Laboratory (LBNL), 1 Cyclotron Road, Berkeley, CA 94720, USA

### Abstract

The NTX experiment at the Heavy Ion Fusion Virtual National Laboratory is exploring the performance of neutralized final focus systems for high perveance heavy ion beams. We are developing a non-destructive beam diagnostic system to characterize the ion beam during its operation. Ion beam space charge is sensed by measuring deflection of mono energetic electron passing transversely through the ion beam. In this diagnostic system an electron beam of a submillimeter size with 1-5  $\mu\text{A}$  current and 5-8 kV energy will be injected perpendicularly through the ion beam. The position and intensity of the deflected e-beam would be registered on a scintillator for optical analysis to characterize the ion beam. An electron beam of negligible space charge will be deflected at an angle that depends on the charge density and energy distribution of the ion beam along its trajectory. The e-beam current and energy are chosen such that its trajectory will be significantly perturbed without perturbing the ion beam. We present a progress report on this diagnostic system including the characterization of the electron gun, the design of the e-beam transport system, and a study of the scintillator and its associate electronics and photonic components.

### INTRODUCTION

The Heavy Ion Fusion program [1] has a great demand for energy production and a series of experiments [2-4] are under way. These experiments have been considering a beam from an ion source, like  $k^+$  [5-6]. When attempting to characterize the profile and field distribution of an ion beam, most diagnostics like a faraday cup, slit cup, pepperpot [7-8], optical scintillator are destructive to the beam line and significantly alter the properties of ion beam itself. Moreover, during the characterization process, a beam line is non-useful for its applications, and characterization is not in same sequence of time of beam application. We are interested in use of an electron beam as an electron probe within a system to develop a non intercepting diagnostic for a ion beam profile and fields measurement.

In this proceeding, overview of the diagnostic design concept will be presented first, and will follow to a description of design, construction and setup of the system. Finally the results of electron beam deflection by magnets and future plan will be presented.

\*This work has been performed under the auspices of the US DOE by UC-LBNL under contract DE-AC03-76SF00098, for the Heavy Ion Fusion Virtual National Laboratory. <sup>#</sup>PKRoy@lbl.gov

### OVERVIEW OF NON-INTERCEPTING DIAGNOSTIC

By measuring the deflections of electrons, from an e-gun, after they pass through an ion beam, we hope to work backwards and quantify how the charge varies throughout the ion beam. In order to create an array of deflections corresponding to every section of the ion beam, the electron beam's initial displacement must be varied. A chicane magnetic arrangement would provide this initial displacement. Figure 1 shows a schematic diagram of the arrangement. This arrangement consists of four dipole magnets (D1 to D4) of equal strength wired in series to produce the field directions shown.

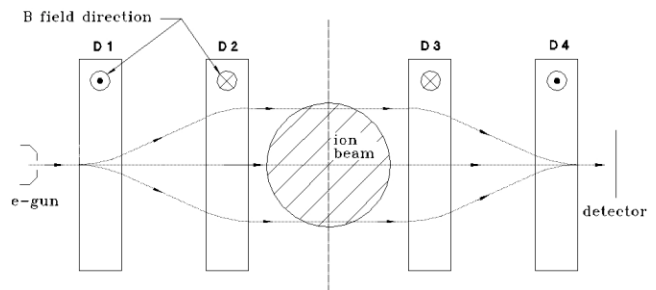


Figure 1: A sketch of non-intercepting beam diagnostic.

By varying the strength of the magnetic fields in a series of measurements, electron beam would be able to pass through every part of the ion beam, and thus a charge distribution of the cross section of the ion beam could be produced. For measurement of e-beam deflection a scintillating detector is placed at the end of the diagnostic. Deflection of an e-beam in an Ion beam charge distribution is calculated using the following formula based on a uniform cylindrical ion charge distribution.

$$\theta = \frac{2J_0 q a b}{v^2 \epsilon_0 m_e} \left( \cos^{-1} \left( \frac{b}{a} \right) \right)^2 \quad (1)$$

where  $J_0$  is the charge density of the ion beam,  $a$  and  $b$  are the ion beam radius, and electron beam displacement by the magnets (D1 and D2), respectively.  $q$ ,  $m_e$  and  $v$  are the charge, mass and velocity of of an electron, respectively.  $\epsilon_0$  is the permittivity of free space. Figure 2 shows a calculated deflection curve for a 5 keV e-beam passing through a 300 keV ion beam of 2 cm diameter and 20 mA current.

## INSTRUMENTATION AND EXPERIMENTAL SETUP

Development of the diagnostic was considered in several stages. These were: selection of electron gun and electron beam imaging scintillator, design of 4 dipole magnets, installation of electron gun, magnets and scintillator in a same vacuum chamber keeping a pathway for a future ion beam line. A brief description of the devices has been presented below.

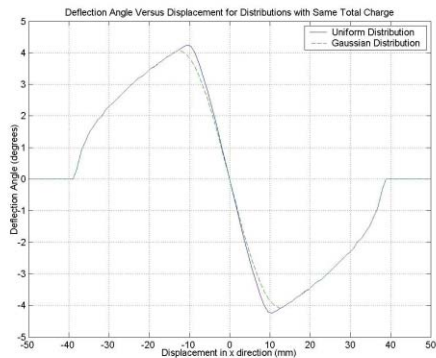


Figure 2: Deflection of electron beam by an ion beam.

### Electron gun

A factory made (EGG-3101, Kimball Physics Inc.) 10 keV, and 10  $\mu$ A range LaB<sub>6</sub> cathode [9-10] embedded electron gun was installed in the diagnostic box to use as an electron probe. A working distance of the gun is around 1 meter with a spot of couple of hundred micron in diameter.

### Chicane Magnet

The dipoles are iron dominated to minimize current requirement and provide high field uniformity. They are designed to operate in vacuum, in order to eliminate the need for a vacuum chamber that can fit between the poletips. Aluminum can be hard anodized for electrical insulation, eliminating the need for organic or fiber base inorganic insulation which are less vacuum compatible. A low current density minimizes resistive loss, allowing coil cooling by radiation only, eliminating the need for water cooling in vacuum. A small number of turns minimize voltage drop and conducting area. This place is less demand on electrical insulation and reduces out gassing. Figure 3 and 4 show the H dipole DC magnet that was designed and fabricated at LBNL. Coils are machined from a single piece of 6060-T6 aluminum, slotted to provide the desired current path, then hard anodized for electrical insulation. Leads are gold plated to minimize contact resistance. Use of annealed ultra low carbon steel was used for high permeability and low out gassing. The magnet layout (30 mm magnetic length along e-beam, 6 mm poletip gap, 60 mm drift distance (horizontal) between steel yokes, 150 mm pole-tip heights) requires a current of 6.7A @ ~3 mV/coil to achieve an e-beam (5 keV) height of 40 mm (32 G). This calculation includes a

PANDIRA [11] derived correction factor for the "bonus" fringe field that provides additional vertical bending beyond the pole-tip edge.

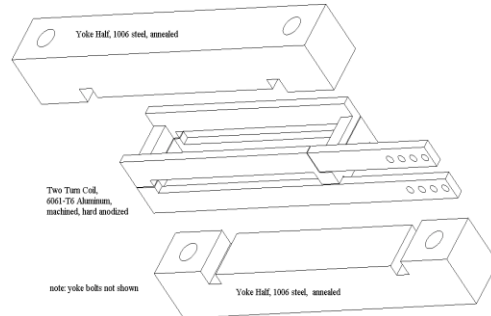


Figure 3: DC dipole magnet, exploded view.

### Scintillator

An Yttrium Aluminum Perovskite Scintillator (YAP:Ce) was used with the system. Density, maximum emission length, decay time and photon emission ability of this scintillator are 5.57 g/cm<sup>3</sup>, 350 nm, 27 nsec, and 18/keV, respectively. It has negligible thermal expansion (4-11 ppm) with high melting point (1875°C). The depth or thickness of the 5 keV stopping at YAP was calculated to be 0.028  $\mu$ m using well known Bethe formula [12], where atomic density of the scintillator in atoms per cubic meter,  $\rho = 3.859 \times 10^{28} \text{ m}^{-3}$  was calculated from a consideration of effective atomic number 36 of YAP:Ce scintillator. This atomic number is equal to atomic number of Krypton (Kr), therefore the atomic mass of YAP is considered to be the same as Kr (83.80). Though a calculated time constant was obtained in the femto second range, however, charge can build up on the front surface of the scintillator, if it is isolated from the ground. This charge buildup will repulse the incoming beam trajectories on or near the same landing area. To drain this charge, a 100 nm Aluminum coating on a YAP scintillator was made by evaporation. The capacitance of scintillate embedded charge relative to the aluminum layer is calculated to be  $5.28 \times 10^{-7}$  farad. An RC time constant  $2.23 \times 10^{-13}$  sec was calculated for the 100 nm coating which is sufficient for charge draining. Some input energy of the e-beam is lost in this coating. For a 100 nm coating this is calculated to be approximately 1.2keV.

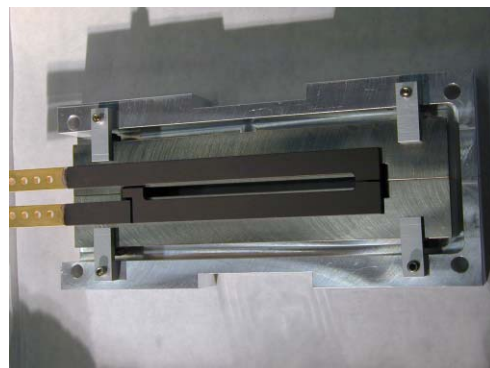


Figure 4: Mechanical Design of a DC dipole magnet.

*Experimental setup*

Figure 5 shows an image of the diagnostic box assembled with an electron gun, magnets and scintillator. A CCD camera is installed and focused on the scintillator. This camera was connected to a computer to record image data. During start up, the gun source is electrically heated to an emission temperature. The electron beam is focused to the scintillator using appropriate voltages for focus and grid. Pressure of the system is maintained better than  $1 \times 10^{-7}$  Torr using 2 turbo-molecular pumps.

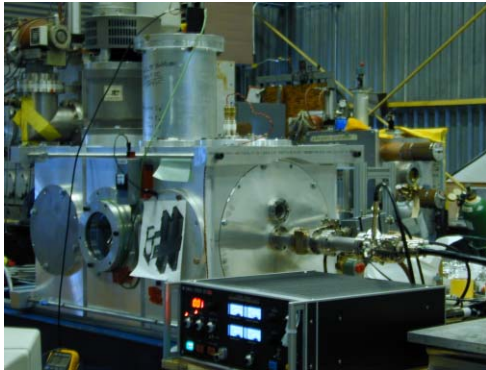


Figure 5: Ion beam diagnostic.

**RESULTS AND DISCUSSIONS**

The electron gun operates at energy of 5 to 10 keV and delivering a beam current as our requirement of 1 to 2  $\mu\text{A}$ . We are able to obtain mm size electron beam spot at a distance of 1.25m (after D4 magnet in the Fig. 1) without any magnetic steering or focusing in the drift path. Figure 6 shows images of electron beam height at an ion beam path (between D2 and D3 of Fig 1.) varying current through magnets D1 and D2 (Fig.1). A small change in electron beam location was identical by knowing a pixel

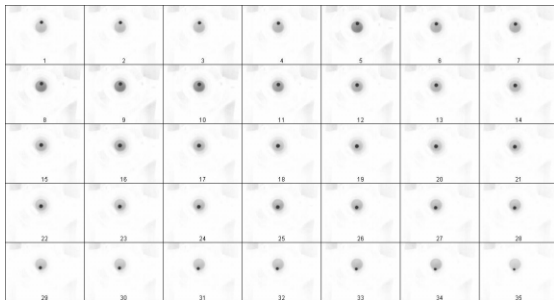


Figure 6: Electron beam deflection height through a 2 cm scintillator. Dark center spot is an e-beam spot deflected from up to down as shown by numerical numbers.

value of the center of an e-beam spot, thus beam size did not effect to any small deviation of landing, and thus were able to get a good resolution of displacement. Figure 7 shows an experimental data of e-beam displacement at the center of the diagnostic (between D2 and D3 in the Fig. 1)

by 2 magnets (D1 and D2). A displacement of 25mm for a 6keV e-beam was recorded by a gap field of 25G or a current of 6.5A through the DC magnets. We measure a height change of  $\pm 3$  cm of the e-beam that indicates that a large size (~6 cm diam.) ion beam scan is possible.

We are designing a time e-beam pulse system to implement the diagnostic in an ion beam.

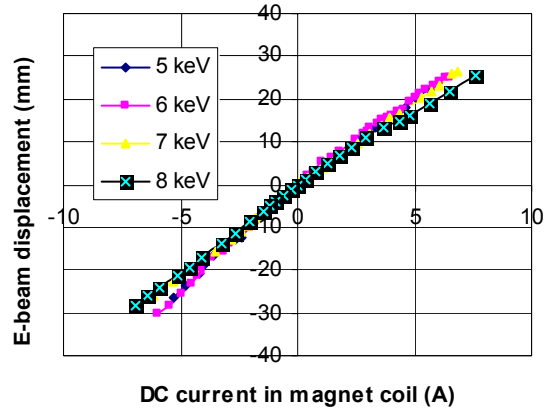


Figure 7: E-beam deflection at the center of diagnostic.

**REFERENCES**

- [1] R.O. Bangerter, "The heavy ion fusion program in the USA" Nucl. Instrum. and Meth. In Phys. Research A, 464 (2001) 17-23.
- [2] S. S. Yu et al., "Focusing and Neutralization of Intense Ion Beams", Proc. PAC '03, TOAA001.
- [3] E. Henestroza et al., "Neutralized Transport of High Intensity Beams", Proc. PAC '03 , WPPG014.
- [4] P.A. Seidl et al., "The high current experiment: First results", Laser and Particle Beams 20 (2002),435-440.
- [5] D. Baca et al., "Fabrication of Large Diameter Alumino-Silicate  $\text{K}^+$  Sources, Proc. PAC '03 FPAB005.
- [6] S. Eylon et al., "High brightness potassium source for the HIF neutralized transport experiment", Proc. PAC '03, WPPG012.
- [7] C. Lejeune et al., "Applied charged particle optics", ed. by A. Septier (1980), pt 13A, 159.
- [8] J. G. Wang et al. Nucl. Instrum. Methods. A307 (1991), 190
- [9] J.M. Lafferty, J. Appl. Phys. 22 (1951), 299.
- [10] P.K.Roy et al., Rev. of Sci. Instrum. 67(12) (1996), 4098.
- [11] K. Halbach et al., POISSON/ SUPERFISH, v 6.28, Los Alamos Accelerator code group, LANL.
- [12] [www.aps.anl.gov/techpub/lsnotes/ls165/ls165/html](http://www.aps.anl.gov/techpub/lsnotes/ls165/ls165/html)